GEOLOGICAL SURVEY OF CANADA
OPEN FILE 7853

Targeted Geoscience Initiative 4: Contributions to the Understanding of Volcanogenic Massive Sulphide Deposit Genesis and Exploration Methods Development

Mineralogical, sulphur, and lead isotopic study of the Lemarchant Zn-Pb-Cu-Ag-Au-VMS deposit: Implications for precious-metal enrichment processes in the VMS environment

Shannon B. Gill[1], Stephen J. Piercey[1], Daniel Layton-Matthews[2], Graham D. Layne[1], and Glenn Piercey[3]

[1]Memorial University of Newfoundland, St. John's, Newfoundland and Labrador
[2]Queen's University, Kingston, Ontario
[3]MicroAnalysis Facility, CREAIT Network, Memorial University of Newfoundland, St. John's, Newfoundland and Labrador

2015

Recommended citation

Gill, S.B., Piercey, S.J., Layton-Matthews, D., Layne, G.D., and Piercey, G., 2015. Mineralogical, sulphur, and lead isotopic study of the Lemarchant Zn-Pb-Cu-Ag-Au-VMS deposit: Implications for precious-metal enrichment processes in the VMS environment, *In:* Targeted Geoscience Initiative 4: Contributions to the Understanding of Volcanogenic Massive Sulphide Deposit Genesis and Exploration Methods Development, (ed.) J.M. Peter and P. Mercier-Langevin; Geological Survey of Canada, Open File 7853, p. 183–195.

TABLE OF CONTENTS

Mineralogical, sulphur, and lead isotopic study of the Lemarchant Zn-Pb-Cu-Ag-Au-VMS deposit: Implications for precious-metal enrichment processes in the VMS environment

Shannon B. Gill[1]*, Stephen J. Piercey[1]†, Daniel Layton-Matthews[2], Graham D. Layne[1], and Glenn Piercey[3]

[1]Department of Earth Sciences, Memorial University of Newfoundland, St. John's, Newfoundland and Labrador A1B 3X5
[2]Department of Geological Sciences and Geological Engineering, Queen's University, Kingston, Ontario K7L 3N6
[3]MicroAnalysis Facility, CREAIT Network, Memorial University of Newfoundland, St. John's, Newfoundland and Labrador A1B 3X5
*Corresponding author's e-mail: s.gill@mun.ca
†Corresponding author's e-mail: spiercey@mun.ca

ABSTRACT

The Lemarchant deposit is a Cambrian volcanogenic massive sulphide (VMS) deposit located in the Central Mobile Belt of the Newfoundland Appalachians. Unlike other polymetallic VMS deposits in the bimodal felsic Tally Pond group, Lemarchant is enriched in precious metals. The deposit is composed of contrasting styles of sulphide mineralization, and formed in three discrete stages: *Stage 1:* barite-rich, low-temperature (<250ºC) VMS mineralization; *Stage 2:* 150 to 250ºC intermediate- to high-sulphidation epithermal-style mineralization; and *Stage 3*: polymetallic, high-temperature (>300ºC) VMS mineralization. Sulphur isotopes suggest that S is derived from three sources: thermochemically reduced seawater sulphate, leached igneous basement rock, and magmatic SO_2. Lead isotopes indicate that Pb is primarily derived from evolved crustal material, with some input from juvenile volcanic rock (i.e. arc-rift). Precious metals associated with epithermal-style mineralization are consistent with a magmatic contribution to the hydrothermal fluid. Precious metals were precipitated from intermittently boiled fluids, at relatively shallow (<1500 m) water depth.

INTRODUCTION

Although volcanogenic massive sulphide (VMS) deposits with precious metal enrichment have been studied globally (e.g. Huston, 2000; Dubé et al., 2007; Mercier-Langevin et al., 2011), precious metal-bearing VMS deposits in the Newfoundland Appalachians are not well-documented and the cause(s) of enrichment in these deposits is poorly understood. The source(s) of precious metals, the environmental and physiochemical conditions that persist during the formation of a VMS deposit can all influence the degree to which a deposit is enriched in metal, including Au and Ag (Poulsen and Hannington, 1995; Hannington et al., 1999; Huston, 2000; Dubé et al., 2007). The Central Mobile Belt in Newfoundland hosts a large number of VMS deposits, including past and presently producing mines, and non-producing deposits and prospects that range from Cu-rich to polymetallic (Swinden and Kean, 1988; Piercey and Hinchey, 2012); a number of these deposits are also precious metal-enriched (e.g. Santaguida and Hannington, 1993, 1996; Pilote and Piercey, 2013; Pilote et al., 2014; Brueckner et al., 2014). The Zn-Pb-Cu-Ag-Au Lemarchant VMS deposit is located in the Tally Pond volcanic belt, together with the currently producing (yet precious metal-poor) Duck Pond and Boundary VMS deposits (Evans and Kean, 2002; McNicoll et al., 2010; Piercey et al., 2014). Lemarchant contains well-preserved sulphide mineral textures and presents an ideal subject for investigating mechanisms of precious metal enrichment in Newfoundland VMS deposits.

The Lemarchant deposit was discovered in 1983, and contains an indicated mineral resource of 1.24 million tonnes grading 5.38 wt% Zn, 0.58 wt% Cu, 1.19 wt% Pb, 1.01 g/t Au, and 59.17 g/t Ag and an inferred mineral resource of 1.34 million tonnes grading 3.70 wt% Zn, 0.41 wt% Cu, 0.86 wt% Pb, 1.00 g/t Au, and 50.41 g/t Ag (Fraser et al., 2012). Herein, we present detailed petrographic and in situ trace and isotope mineral chemical data for the Lemarchant deposit collected using a combination of scanning electron microscopy (SEM), electron microprobe (EMPA), laser ablation

Gill, S.B., Piercey, S.J., Layton-Matthews, D., Layne, G.D., and Piercey, G., 2015. Mineralogical, sulphur, and lead isotopic study of the Lemarchant Zn-Pb-Cu-Ag-Au-VMS deposit: Implications for precious-metal enrichment processes in the VMS environment, *In:* Targeted Geoscience Initiative 4: Contributions to the Understanding of Volcanogenic Massive Sulphide Deposit Genesis and Exploration Methods Development, (ed.) J.M. Peter and P. Mercier-Langevin; Geological Survey of Canada, Open File 7853, p. 183–195.

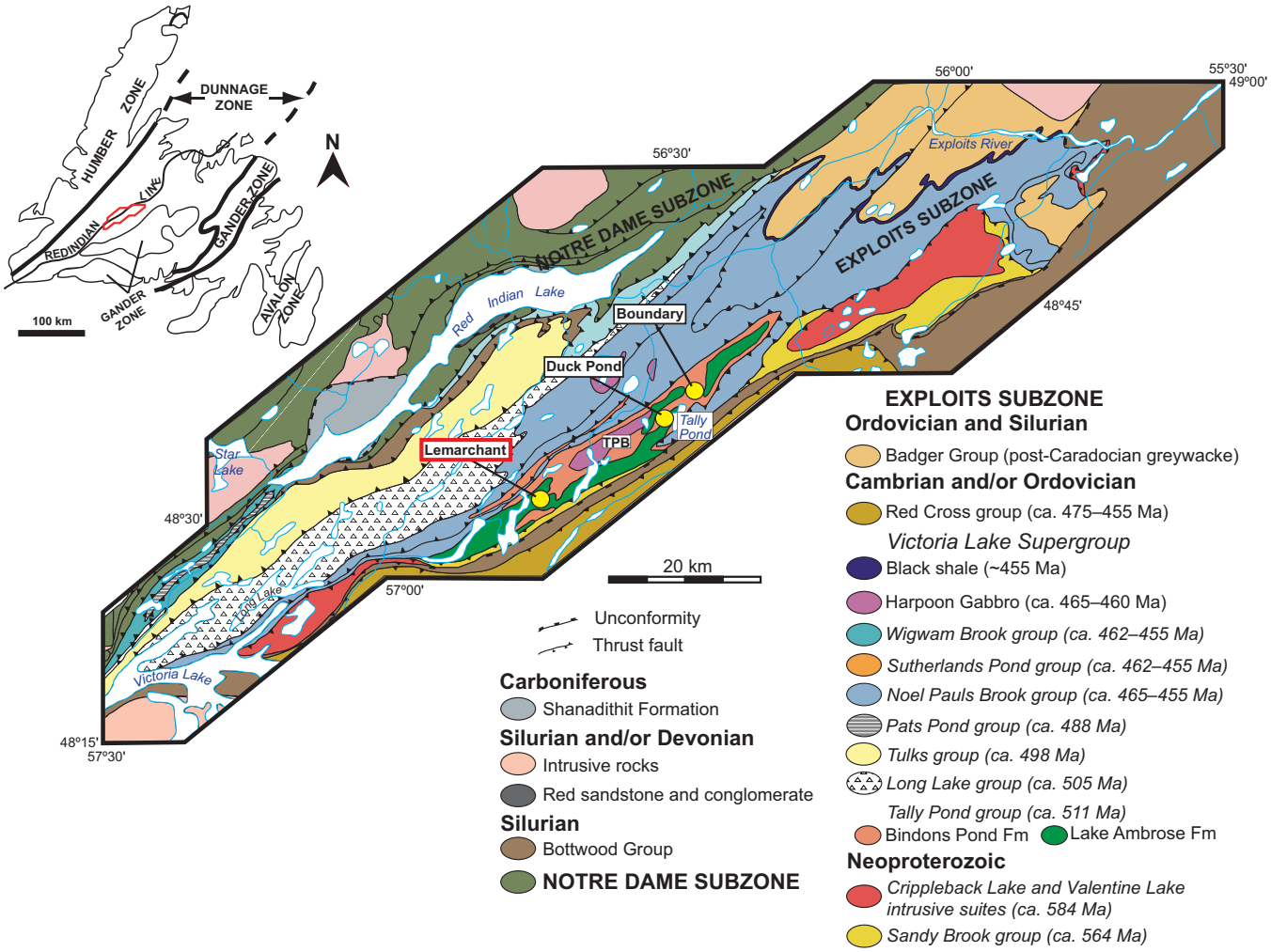

Figure 1. Geological map of the volcanic sequences comprising the Exploits subzone, eastern Dunnage Zone. The Tally Pond volcanic belt (TPB) is host to the Lemarchant VMS deposit (in red), Duck Pond and Boundary VMS deposits. Modified from Rogers et al. (2006), McNicoll et al. (2010), and Piercey and Hinchey (2012). Inset map (Williams, 1979) outlines the 4 tectonostratigraphic zones of the Newfoundland Appalachians; map area of Exploits subzone is outlined in red.

inductively coupled plasma (LA-ICP-MS), and secondary ion mass spectrometry (SIMS). The goal of this project is to provide a model for the mineralogical and metallogenic evolution of the Zn-Pb-Cu-Ag-Au Lemarchant deposit. We present here a summary of the work completed to date, and a genetic model for the Lemarchant deposit (and similar deposits elsewhere) that explains the enrichment of precious metals in VMS deposits.

GEOLOGICAL SETTING

Most VMS deposits in the Newfoundland Appalachians are situated within the Dunnage Zone, the central tectonostratigraphic zone of the Newfoundland Appalachians. The Dunnage Zone hosts a suture zone (Red Indian Line, Fig. 1 inset) between volcanic arc sequences of Laurentian and Gondwanan affinity that merged during the Silurian closure of the Iapetus Ocean (Williams, 1979; van Staal et al., 1998; van Staal and Barr, 2012). The eastern, peri-Gondwanan portion of the Dunnage Zone, the Exploits subzone, consists of a series of nascent to mature volcanic arc rocks that include the Victoria Lake Supergroup (Fig. 1; Rogers et al., 2006; Zagorevski et al., 2007). The oldest sequence in the Victoria Lake Supergroup is the 513–509 Ma Cambrian Tally Pond group (Pollock, 2004; Rogers et al., 2006; McNicoll et al., 2010), which is composed of the mafic volcanic-dominated Lake Ambrose formation and the felsic volcanic-dominated Bindons Pond formation (Dunning et al., 1991; Evans and Kean, 2002; Squires and Moore, 2004; Rogers et al., 2006).

The volcanic rocks hosting VMS mineralization in the Tally Pond group are predominantly felsic (Fig. 2a; McNicoll et al., 2010); the Lemarchant VMS deposit, in particular, has been well preserved despite regional greenschist facies metamorphism, folding, and local normal and thrust faulting (Squires and Moore, 2004; Copeland et al., 2008a,b; Fraser et al., 2012). Footwall

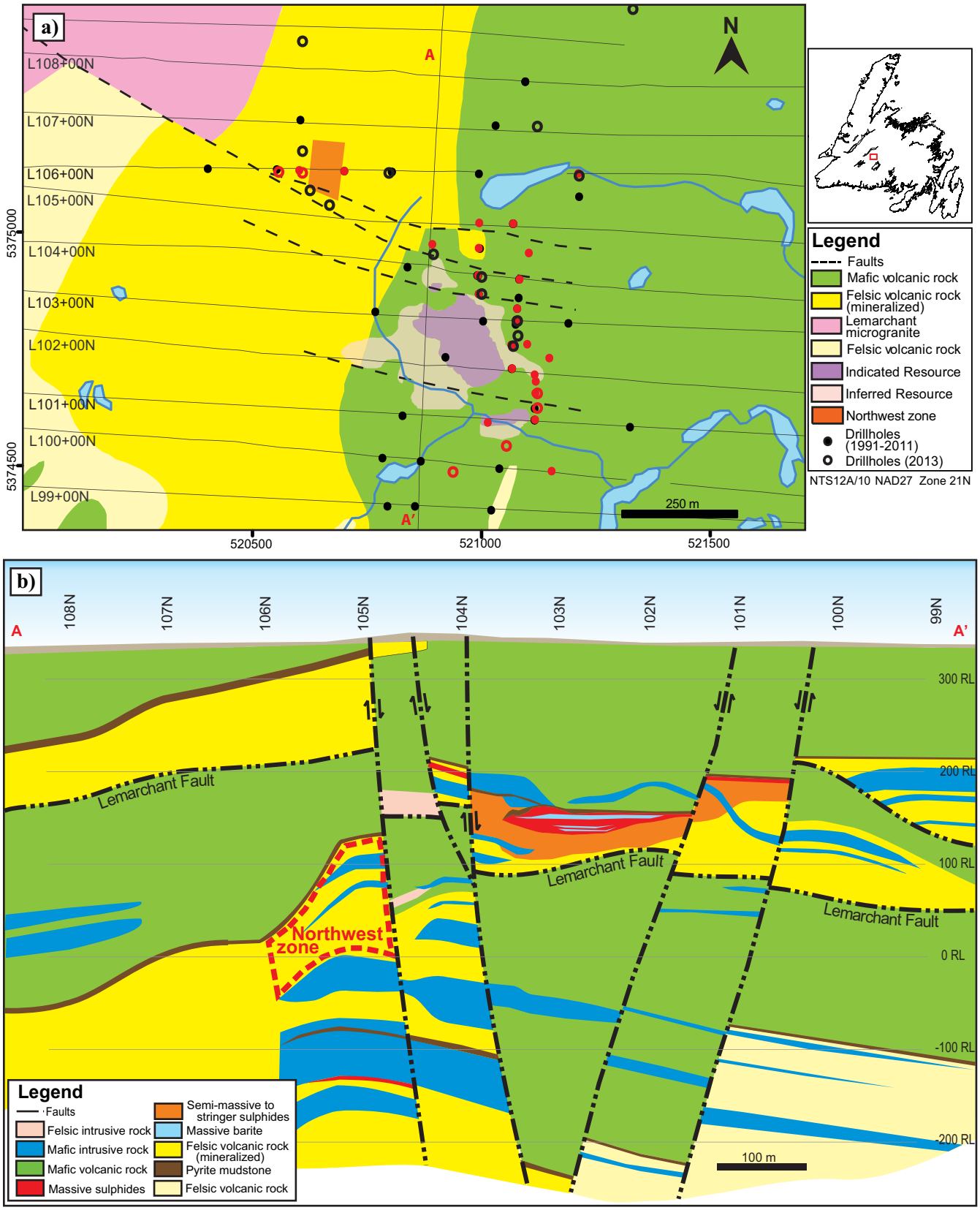

Figure 2. Geology of the Lemarchant deposit. **a)** Surface geology map of Lemarchant deposit. Red drillholes were logged for this project, and section A-A' is marked in red. Map location is approximated in inset map of Newfoundland (Williams et al., 1979). **b)** Idealized north-south cross-section of the Lemarchant deposit, looking east. Modified from Fraser et al. (2012).

host rocks at Lemarchant consist of calc-alkaline aphyric rhyolite breccias and flows that are interbedded with tuff breccias and lapilli tuffs containing devitrified volcanic glass shards (hyaloclastite). Hanging wall rocks consist of basalt and basaltic andesite flows and pillow flows that are variably intercalated with pyritic to graphitic mudstone that has a significant exhalative (chemical sedimentary) component (Lode et al., 2014; Fig. 2b). Two types of mafic dykes, a synvolcanic, pyroxene-porphyritic type and an undeformed gabbroic type, as well as an undeformed felsic dyke, crosscut the Lemarchant host rock and mineralization (Copeland et al., 2008a,b; Fraser et al., 2012). Thrust faulting at Lemarchant has resulted in local repetition of the volcanic stratigraphy (Fig. 2b).

Hydrothermal alteration is manifested by quartz-sericite±chlorite-albite in the footwall host rock, and by weak quartz-chlorite±epidote in the hanging wall (Copeland et al., 2008a,b). Synvolcanic mafic dykes contain rare fuchsite. Late carbonate alteration, consisting of calcite, ankerite, and dolomite, is present in all lithologies, and crosscutting quartz-carbonate veinlets are common throughout the deposit.

Table 1. Ore-related minerals present in the Lemarchant deposit, with mineral formulas (where applicable), in order of decreasing relative abundance.

Mineral phase	Formula
Barite	$BaSO_4$
Sphalerite	(Zn,Fe)S
Pyrite	FeS_2
Galena	PbS
Chalcopyrite	$CuFeS_2$
Tetrahedrite group minerals	$(Cu,Ag)_{10}(Fe,Zn)_2(As,Sb)_4S_{13}$
Bornite	Cu_5FeS_4
Marcasite	FeS_2
Stromeyerite	AgCuS
Colusite group minerals	$Cu_{26}V_2(As,Ge,Sb,Sn)_6S_{32}$
Pyrrhotite	$Fe_{1-x}S$
Arsenopyrite	FeAsS
Covellite	CuS
Electrum	(Au,Ag)
Bournonite	$PbCuSbS_3$
Polybasite	$[(Ag,Cu)_6(Sb,As)_2S_7][Ag_9CuS_4]$
Miargyrite	$AgSbS_2$
Silver telluride	-----
Sulvanite	$Cu_3(V,Fe)S_4$
Reinerite	$(Cu,Fe)_{22}(Ge_{4-x}As_x)Fe_8S_{32}$
Nickel sulphide	-----

SULPHIDE MINERALOGY

The elongate Lemarchant deposit is (at ~200 m depth) 350 m long, <20 m thick, and strikes north-northwest (Fig. 2). The upper stratigraphic stratiform zone contains abundant barite mineralization and is dominated by Zn-Pb sulphides, whereas the lower stratigraphic stringer zone is mostly composed of Cu-rich sulphides. However, the Lemarchant thrust fault (Fig. 2b) has truncated the stringer zone and translocated a portion of the deposit to the northwest (Fig. 2a). The main sulphide minerals are sphalerite, pyrite, galena, and chalcopyrite (see Table 1). Minor sulphide and sulphosalt minerals include the tetrahedrite group minerals, bornite, marcasite, stromeyerite, colusite group minerals, pyrrhotite and arsenopyrite. Trace minerals include electrum, covellite, bournonite, polybasite, miargyrite, sulvanite, and reinerite, as well as unknown silver tellurides and nickel sulphides.

There are five types of mineralization, based on sulphide mineral textures and crosscutting relationships. The type 1 mineral assemblage is composed of semi-massive granular barite-white to honey sphalerite-colloform pyrite-galena±chalcopyrite-tetrahedrite group minerals (Fig. 3a–c). Type 2A and type 2B mineral assemblages crosscut the type 1 mineral assemblage; type 2A mineralization consists of bornite-galena-chalcopyrite±stromeyerite-covellite-NiS stringers (Fig. 3d, e), and type 2B mineralization contains disseminated

Figure 3 opposite. Drillcore photographs, reflected and transmitted light thin section photomicrographs and back-scatter electron (BSE) images of the type mineral assemblages at Lemarchant. *Type 1:* **a)** Granular barite with semi-massive white sphalerite, pyrite, and galena in drillcore (drillhole LM11-64 at 218.8 m depth). **b)** White sphalerite with chalcopyrite disease in transmitted light (sample CNF29959 in drillhole LM11-59 at 207.7 m). **c)** Colloform pyrite with sphalerite and galena in reflected light (sample CNF29960 in drillhole LM11-59 at 216 m). *Type 2A:* **d)** Bornite-galena-chalcopyrite stringers crosscutting type 1 mineralization in drillcore (drillhole LM11-62 at 259.6 m). **e)** Chalcopyrite infilling fractures in bornite, with galena and diagenetic covellite in reflected light (sample CNF14279 in drillhole LM08-33 at 230.8 m). *Type 2B:* **f)** Recrystallized fine-grained pyrite with growth zones of higher As, visible only in back-scatter electron (BSE) image (lighter grey bands; sample CNF25134 in drillhole LM11-56 at 158.7 m). **g)** Coarse barite-dark grey tetrahedrite-galena-white sphalerite stringers crosscutting type 1 mineralization in drillcore (drillhole LM11-52 at 212.3 m). **h)** Myrmekitic intergrowth of galena-colusite-sphalerite in reflected light (sample CNF14279 in drillhole LM08-33 at 230.8 m). **i)** Electrum associated with galena and massive tetrahedrite in reflected light (sample CNF25121 in drillhole LM11-52 at 212.3 m). **j)** Zoned tetrahedrite-tennantite crystal, highlighting increase in silver content and visible in BSE image (lighter grey bands; sample CNF14293 in drillhole LM11-65 at 161.75 m). *Type 3:* **k)** Massive red sphalerite-euhedral pyrite-galena in drillcore (drillhole LM11-65 at 158.7 m). **l)** Subhedral pyrite atoll with chalcopyrite-galena-sphalerite in reflected light (sample CNF14290 in drillhole LM11-65 at 158.7 m). **m)** Massive red sphalerite with scalloped galena in transmitted light (sample CNF29959 from drillhole LM11-59 at 207.72 m). *Type 4:* **n)** Chalcopyrite-pyrite stringers in rhyolite breccia in drillcore (drillhole LM07-14 at 207.4 m). **o)** Subhedral and euhedral atoll pyrite-chalcopyrite stringers with sphalerite in reflected light (sample CNF29971 in drillhole LM11-63 at 224.7 m). Abbreviations: Ag-Trt = silver-rich tetrahedrite; Ant = anatase; Bn = bornite; Brt = barite; Ccp = chalcopyrite; Col = colusite; Cv = covellite; Elec = electrum; Gn = galena; Py = pyrite; Sp = sphalerite; Tnn = tennantite; Trt = tetrahedrite.

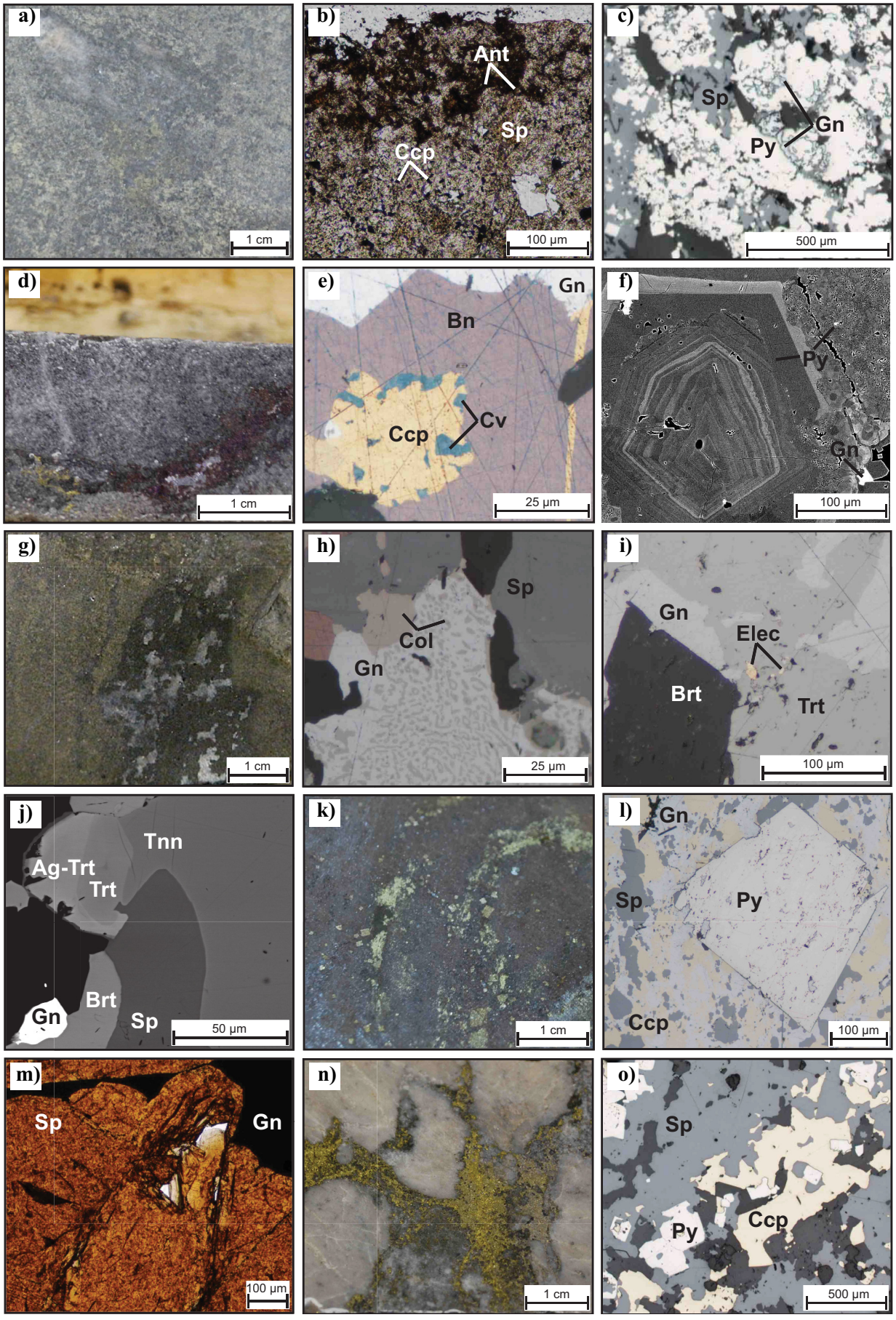
a)
1 cm
b)
Ant
Sp
Ccp
100 µm
c)
Sp
Gn
Py
500 µm
d)
1 cm
e)
Gn
Bn
Cv
Ccp
25 µm
f)
Py
Gn
100 µm
g)
1 cm
h)
Sp
Col
Gn
25 µm
i)
Gn
Elec
Brt
Trt
100 µm
j)
Tnn
Ag-Trt
Trt
Brt
Gn
Sp
50 µm
k)
1 cm
l)
Gn
Sp
Py
Ccp
100 µm
m)
Sp
Gn
100 µm
n)
1 cm
o)
Sp
Py
Ccp
500 µm

tetrahedrite group minerals-galena-bladed barite-white sphalerite-recrystallized pyrite±electrum-colusite group minerals-Ag-tetrahedrite-polybasite-miargyrite-bournonite-AgTe (Fig. 3f–j). Type 3 massive honey-brown to red sphalerite-subhedral to euhedral pyrite-galena-chalcopyrite± pyrrhotite-arsenopyrite overprints the type 1 assemblage in the uppermost portion of the stratiform zone (Fig. 3k–m). The type 4 mineral assemblage occurs in the stringer zone as chalcopyrite-euhedral pyrite± orange sphalerite-galena stringers (Fig. 3n, o).

MINERAL CHEMISTRY

Samples of representative mineral species and sulphide textures were analyzed using a scanning electron microprobe (SEM) equipped with an energy dispersive X-ray (EDX) detector, and quantitative compositions of sulphide and sulphosalt phases (see Table 1) were obtained by wavelength dispersive spectroscopy (WDS) using electron microprobe analysis (EMPA). Elemental precision for major elements is <1% (1σ); minor element (<1 wt%) precision is lower, with detection limits between 100–500 ppm (3σ). Semi-quantitative determinations of trace elements in sulphide and sulphosalt grains >50 μm were obtained via laser ablation inductively-coupled plasma mass spectrometry (LA-ICP-MS), on a 193 nm Excimer laser and quadropole mass spectrometer following the methods outlined by Longerich et al. (1996) and Eggins et al. (1998). Internal calibration was performed using USGS standards (to R >0.95) and compared to recommended values for the external standard (less than 20% error for trace elements <10 ppm).

Minor and Trace Element Geochemistry

Microprobe results reveal variations in minor element and precious metal contents in sphalerite, pyrite, tetrahedrite group minerals, bornite, and electrum phases. Iron contents of sphalerite range from below detection limit to 8.4 wt% (7.4 mol%), and correspond to variations in sphalerite colour—white to honey sphalerite (Fig. 3b) from type 1, 2A, and 2B assemblages contains Fe <2.6 wt% (<2.3 mol%), whereas honey brown to red sphalerite (Fig. 3m) from the type 3 and 4 assemblages has 2.7–8.4 wt% Fe (2.4–7.4 mol%) (Fig. 4). Arsenic contents in zoned pyrite (Fig. 3f) range up to 3.6 wt%. Tetrahedrite group minerals range from end-member tennantite to end-member tetrahedrite, and Ag is positively correlated with Sb, which is consistent with the fractional crystallization model of Hackbarth and Petersen (1984) and Huston et al. (1996) for tetrahedrite. Silver-tetrahedrite (i.e. friebergite) is distinct from tetrahedrite and is significantly enriched in Ag (15–28 wt%; see Fig. 3j). Silver also occurs in stromeyerite, electrum, polybasite, miargyrite, and

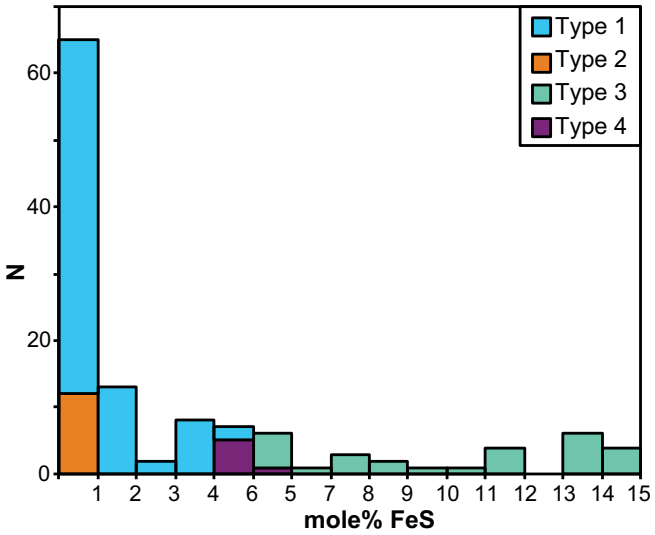

Figure 4. Compositional variation in iron contents (mol% FeS) of sphalerite from sphalerite-bearing mineral assemblages in the Lemarchant deposit (data from electron microprobe analyses).

AgTe, and in trace amounts in bornite (<1.5 wt%). Gold occurs primarily in electrum, which is predominant in the centre of the deposit as Au-rich electrum (Au:Ag > 0.7). Ag-bearing minerals and Ag-rich electrum (Au:Ag = 0.4 to 0.7) are more abundant toward the edges of mineralization.

Laser ablation ICP-MS analyses reveal distinct variations in trace element contents between the five type mineral assemblages (e.g. Au, Bi, In, Sn; Fig. 5). The type 1 mineral assemblage is enriched in As, Mo, and Tl relative to the other mineral assemblages. The type 2A mineral assemblage is enriched in Ag, Ge, and Sn, and the type 2B mineral assemblage is enriched in V, In, Au, and Sb; both assemblages contain elevated Bi, Cr, Co, In, Ni, and Ti. The type 3 assemblage is also enriched in Ni. The type 4 assemblage has low trace element contents relative to the other assemblages, with the exception of Sn.

ISOTOPE GEOCHEMISTRY

Offcuts from thin sections analyzed by SEM, EMPA, and LA-ICP-MS were mounted in epoxy and gold-coated for in situ isotope analyses by secondary ion mass spectrometry. Grains with unblemished spots >10 μm were chosen (where possible) in galena, pyrite, and chalcopyrite that were representative of the five types of mineralization. Precision, based on an internal galena standard for radiogenic isotope ratios ($^{204}Pb/^{206}Pb$, $^{207}Pb/^{206}Pb$, and $^{208}Pb/^{206}Pb$), is better than 0.05–0.10% (1σ). Repeated analyses on galena standards indicate accuracy is better than 0.10–0.15% (1σ). Internal precision of $\delta^{34}S$ analyses on pyrite, galena, and chalcopyrite standards is ±0.3‰ (1σ), and accuracy of repeated standard analyses is better than

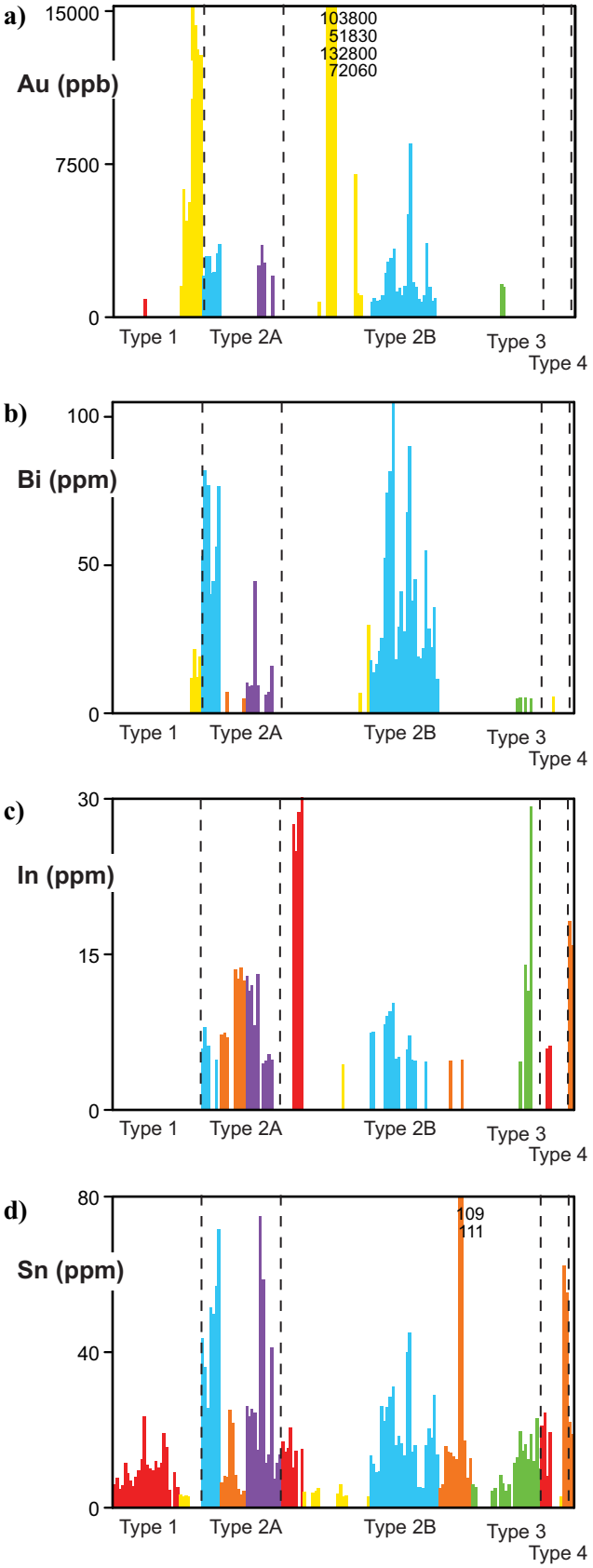

Figure 5. Trace element variations in sphalerite (red), pyrite (yellow), chalcopyrite (orange), galena (blue), tetrahedrite (green), and bornite (purple) from the five types of mineralization at the Lemarchant deposit.

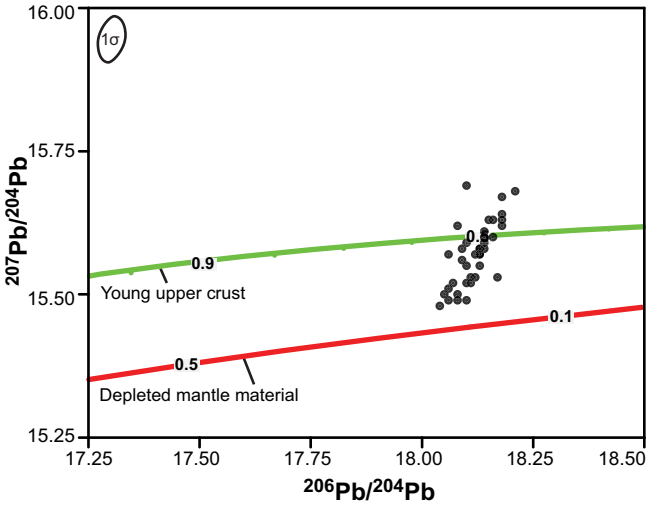

Figure 6. $^{207}Pb/^{204}Pb$ versus $^{206}Pb/^{204}Pb$ plot of galena from the Lemarchant deposit. Error ellipse for average standard deviation (1σ) does not include outlying values. Young upper crust and depleted mantle material growth curves from Kramers and Tolstikhin (1997).

±0.35–0.45‰ (1σ).

Lead Isotope Geochemistry

Lead isotope compositions of galena from Lemarchant form a linear array on a $^{207}Pb/^{204}Pb$ versus $^{206}Pb/^{204}Pb$ plot (Fig. 6; n=42). Model ages and μ values calculated using the two-stage growth model of Stacey and Kramers (1975) give Pb-Pb ages that are much younger than Cambrian (509–513 Ma, as determined by U-Pb dating of the Lemarchant host rocks; Pollock, 2004; Rogers et al., 2006; McNicoll et al., 2010) and an average μ of 9.63. These μ values are very similar to the μ value for young upper crust at 500 Ma (μ=9.66; Kramers and Tolstikhin, 1997), which is consistent with the volcanic and intrusive Neoproterozoic basement rock that has a dominant continental arc signature (εNdt<0; Rogers et al., 2006; McNicoll et al., 2010) and immediately underlies the Tally Pond group. However, the spread of data, which lie mostly below the young upper crust growth curve (Fig. 6), suggest that an additional source with low-μ values (i.e. juvenile Pb from mafic rocks of the lower Neoproterozoic basement or Lake Ambrose formation; Rogers et al., 2006; McNicoll et al., 2010) must have contributed to the Pb isotope signature at Lemarchant.

Sulphur Isotope Geochemistry

Sulphur isotope compositions of Lemarchant sulphides reveal a relatively wide range of $\delta^{34}S$ values between -6.4 and +15.1‰ (avg. +5.0 ± 3.3 ‰, n = 119). Sulphur isotope values ~0‰ occur in type 2A pyrite (+1.4 ± 2.2‰), type 2B galena (+4.4 ± 4‰), and type 3 galena (+4.5 ± 6.6‰), whereas the highest $\delta^{34}S$ values are from galena in the type 3 (<+15.1‰) and type 4 (+7.2 ± 4.2‰) assemblages (Fig. 7).

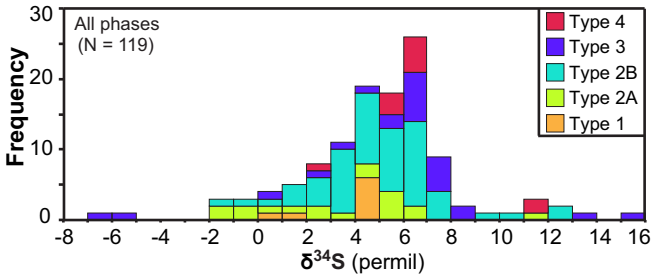

Figure 7. Frequency distribution of $\delta^{34}S$ values for all analyzed sulphides (pyrite, galena, and chalcopyrite) from the 5 mineral assemblage types at the Lemarchant deposit.

SUMMARY

The Lemarchant VMS deposit is composed of contrasting styles of mineralization, which were deposited in three discrete paragenetic stages (Fig. 8). The type 1 mineral assemblage was deposited during stage 1 of paragenesis and contains fine-grained barite and fine-grained polymetallic sulphides, such as low-Fe sphalerite and colloform pyrite that are indicative of transport by low-temperature (200-300ºC), oxidized hydrothermal fluids (Large, 1977; Barton and Skinner, 1979; Ohmoto et al., 1983; Pisutha-Arnond and Ohmoto, 1983; Ohmoto, 1996). The type 1 assemblage was crosscut by the type 2A and 2B mineral assemblages during stage 2 paragenesis, which contain low-Fe sphalerite and abundant sulphosalts, precious metals, and precious metal-bearing sulphides atypical of polymetallic VMS deposits (c.f. Hannington and Scott, 1989; Sillitoe et al., 1996; Dubé et al., 2007); rather, the type 2A and 2B assemblages resemble an intermediate- to high-sulphidation epithermal suite of minerals that were deposited from low-temperature (150–250ºC), oxidized, near neutral (pH ~5) hydrothermal fluids with high sulphur activity (Scott and Barnes, 1971; Czamanske, 1974; Barton and Skinner, 1979; Pisutha-Arnond and Ohmoto, 1983; Hannington and Scott, 1989; Huston and Large, 1989). Paragenetic stage 3 resulted in the overprinting of type 1, 2A, and 2B assemblages in the stratiform zone by the type 3 assemblage, and the formation of a stringer sulphide zone with the type 4 assemblage. The high-Fe sphalerite, high Cu-content, and lack of precious and trace metals in the type 3 and 4 assemblages suggests that these polymetallic, Kuroko-style VMS assemblages were deposited from higher temperature (>300ºC), less oxidized hydrothermal fluids with low sulphur activity (Scott and Barnes, 1971; Barton and Skinner, 1979; Eldridge et al., 1983; Pisutha-Arnond and Ohmoto, 1983; Ohmoto, 1996).

The intermediate- to high-sulphidation epithermal suite of minerals (i.e. tetrahedrite group minerals, bornite, colusite group minerals, electrum, covellite) and epithermal trace element suite (i.e. Au, As, Bi, Co, Cr, In, Mo, Ni, Sb, Se, Te) that characterize the type 2A and 2B assemblages suggest that direct contribution of magmatic fluid to the hydrothermal fluid occurred during the formation of the Lemarchant deposit (Hedenquist and Lowenstern, 1994; Poulsen and Hannington, 1995; White and Hedenquist, 1995;

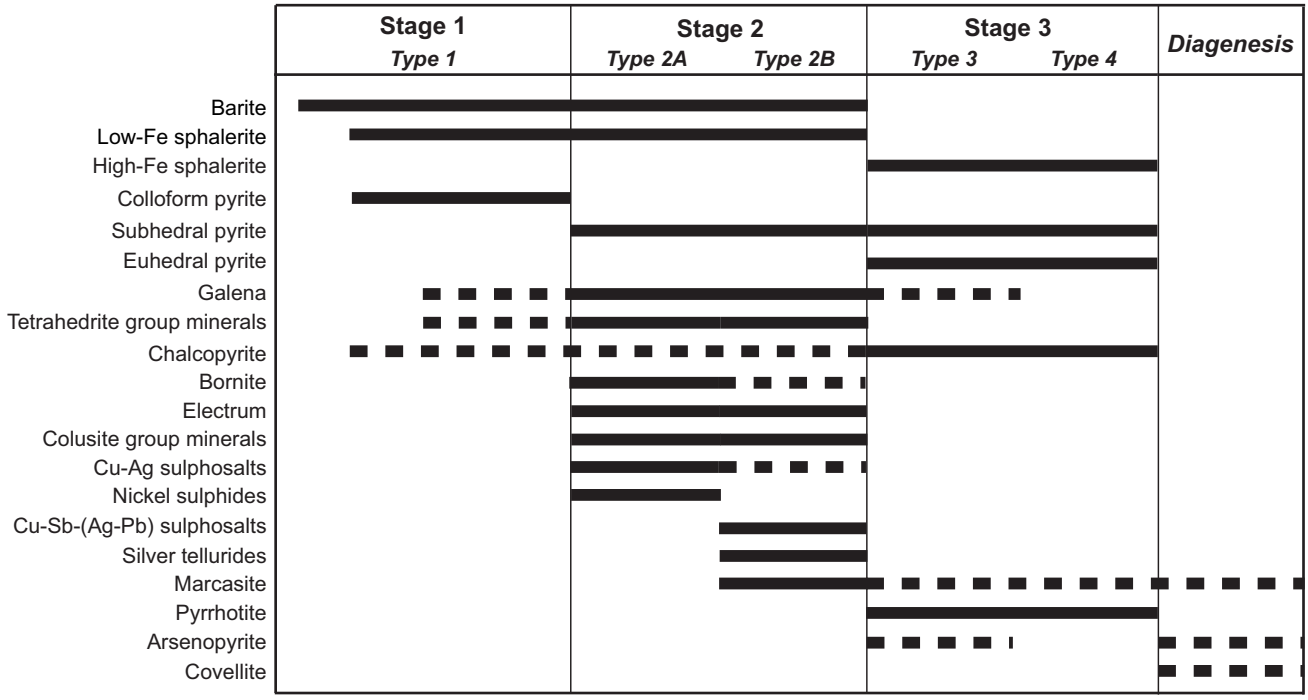

Figure 8. Paragenetic diagram for the three main stages of deposition of the Lemarchant deposit. Dashed lines indicate intermittent deposition of mineral phase.

Lydon, 1996; Sillitoe et al., 1996; Hannington et al., 1999). Magmatic fluids are consistent with the presence of anomalous Au in the deposit, which would have been efficiently transported by the low-temperature, highly oxidized, near neutral and S-rich fluids of stage 1 and 2 paragenesis (Hannington and Scott, 1989; Huston and Large, 1989; Lydon, 1996). Further evidence for a magmatic contribution to the hydrothermal fluid comes from the S isotope signature of the Lemarchant sulphides (Fig. 7; Gill, 2015). Positive $\delta^{34}S$ values (>4‰) indicate that some S at Lemarchant was derived from thermochemical sulphate reduction (TSR; Sakai and Dickson, 1978; Ohmoto and Rye, 1979; Shanks, 2001; Seal, 2006); however, $\delta^{34}S$ values of ~0 suggest that leaching of igneous basement rock and/or magmatic fluids also contributed to the overall S isotope signature at Lemarchant (Sakai et al., 1984; Ueda and Sakai, 1984; Huston, 1999; Franklin et al., 2005). The epithermal mineral and trace element suite, abundance of precious metals, and oxidized state of the type 1, 2A, and 2B assemblages are consistent with a magmatic contribution of S (in the form of SO_2; Ohmoto and Rye, 1979; Seal, 2006) during paragenetic stages 1 and 2. The more 'normal' VMS mineralization of the type 3 and 4 assemblages indicate that magmatic fluids were not as prevalent during paragenetic stage 3, so the very low $\delta^{34}S$ values of the type 3 assemblage must be attributed to leaching of igneous rocks.

Precious metal enrichment of the Lemarchant deposit occurred during stage 2 paragenesis, with transport and precipitation from low-temperature, oxidized, near neutral and S-rich fluids. The association of electrum, bladed barite, and euhedral albite in the type 2B assemblage provides further evidence that Au and Ag were precipitated from hydrothermal fluids that intermittently boiled at or very near the seafloor (Sillitoe et al., 1996; Huston et al., 2000; Dubé et al., 2007; Hannington and Monecke, 2009). Boiling of low-temperature fluids at the seafloor requires that Lemarchant formed in relatively shallow water (<1500 m depth) during Au-Ag deposition (Bischoff and Rosenbauer, 1984; Butterfield et al., 1990; Hannington et al., 1999; Hannington and Monecke, 2009; Monecke et al., 2014). However, the Cu-rich, high-temperature mineral assemblages deposited during paragenetic stage 3 show no evidence for boiling. Furthermore, fluid temperatures >250ºC require confining pressures at >1500 m depth to suppress boiling (and concomitant precious metal deposition), suggesting deposition of the type 3 and 4 assemblages occurred at depths greater than 1500 m (Bischoff and Rosenbauer, 1984; Butterfield et al., 1990; Hannington et al., 1995; Hannington et al., 2005). A change in water depth during deposition of mineralization is consistent with the rifted arc environment in which Lemarchant formed (Fig. 6; Squires and Moore, 2004; Copeland et al., 2008a,b; McNicoll et al., 2010; Monecke et al., 2014; Piercey et al., 2014), where extension of the arc during deposit formation resulted in greater depths of water for the latter stages of mineralization.

Lemarchant is a precious-metal-bearing VMS deposit that contains polymetallic, Kuroko-style mineralization, and intermediate- to high-sulphidation epithermal-style mineralization that is atypical of 'normal' VMS systems that lack precious metal enrichment. Precious metals were likely derived directly from a magmatic fluid; however, precipitation and concentration of Au occurred during boiling of the hydrothermal fluid, which could have occurred only at shallow depths. The precious metal deposition at Lemarchant likely occurred in an extensional tectonic environment, consistent with the rifted arc setting.

ACKNOWLEDGEMENTS

Funding for this project primarily came from the GSC TGI-4 Program and the Research Affiliate Program of NRCan. This research is also supported by grants to Dr. Stephen J. Piercey, including an NSERC Discovery Grant and the NSERC-Altius Industrial Research Chair in Mineral Deposits supported by NSERC, Altius Resources Inc., and the Research and Development Corporation of Newfoundland and Labrador. Access to the Lemarchant drill core, core logs, and assay database were provided by the Canadian Zinc Corporation. Many thanks to Stefanie Lode, Christine Divine, Diane Fost, Michael Schaeffer, David Grant, Brian Joy, and Mike Gadd for their technological help and interpretive guidance. The authors thank Jan Peter and Patrick Mercier-Langevin for reviews and editorial handling.

REFERENCES

Barton Jr, P. and Skinner, B., 1979. Sulphide mineral stabilities, *In:* Geochemistry of Hydrothermal Ore Deposits, 2nd Edition, (ed.) H.L. Barnes; John Wiley & Sons, p. 278–403.

Bischoff, J.L. and Rosenbauer, R.J., 1984. The critical point and two-phase boundary of seawater, 200–500ºC; Earth and Planetary Science Letters, v. 68, p. 172–180.

Brueckner, S.M., Piercey, S.J., Sylvester, P.J., Maloney, S., and Pilgrim, L., 2014. Evidence for syngenetic precious metal enrichment in an Appalachian volcanogenic massive sulfide system: the 1806 zone, Ming mine, Newfoundland, Canada; Economic Geology, v. 109, 1611–1642.

Butterfield, D.A., Massoth, G.J., McDuff, R.E., Lupton, J.E., and Lilley, M.D., 1990. Geochemistry of hydrothermal fluids from Axial Seamount hydrothermal emissions study vent field, Juan de Fuca Ridge: Subseafloor boiling and subsequent fluid-rock interaction; Journal of Geophysical Research: Solid Earth, v. 95, p. 12895–12921.

Copeland, D.A., Toole, R.M.S., and Piercey, S.J., 2008a. Assessment report on diamond drilling and soil sampling, License 8183M (10th Year) and 9569M (5th Year) South Tally Pond property, Rogerson Lake area, Newfoundland and Labrador, NTS 12A/10 and 12A/07; Newfoundland and

Labrador Geological Survey, Assessment Report, 956 p. [for Paragon Minerals and Altius Minerals].

Copeland, D.A., McClenaghan, S.M., and Piercey, S.J., 2008b. Ninth year assessment report on diamond drilling, lithogeochemistry, pulse EM surveying and linecutting on license 8183M, South Tally Pond Property, Rogerson Lake area, Newfoundland and Labrador NTS 12A/10 and 12A/07. Newfoundland and Labrador Geological Survey, Assessment Report, 91 p. [for Paragon Minerals and Altius Minerals].

Czamanske, G.K., 1974. The FeS content of sphalerite along the chalcopyrite-pyrite-bornite sulphur fugacity buffer; Economic Geology, v. 69, p. 1328–1334.

Dubé, B., Gosselin, P., Mercier-Langevin, P., Hannington, M., and Galley, A., 2007. Gold-rich volcanogenic massive sulphide deposits, *In:* Mineral Deposits of Canada: A Synthesis of Major Deposit Types, District Metallogeny, the Evolution of Geological Provinces, and Exploration Methods, (ed.) W.D. Goodfellow; Geological Association of Canada, Mineral Deposits Division, Special Publication, v. 5, p. 75–94.

Dunning, G.R., Swinden, H.S., Kean, B.F., Evans, D.T.W., and Jenner, G.A., 1991. A Cambrian island arc in Iapetus; geochronology and geochemistry of the Lake Ambrose volcanic belt, Newfoundland Appalachians; Geological Magazine, v. 128, p. 1–17.

Eggins, S., Rudnick, R., and McDonough, W., 1998. The composition of peridotites and their minerals: a laser-ablation ICP–MS study; Earth and Planetary Science Letters, v. 154, p. 53–71.

Eldridge, C.S., Barton, P.B., Jr., and Ohmoto, H., 1983. Mineral textures and their bearing on formation of the Kuroko orebodies, *In:* The Kuroko and Related Volcanogenic Massive Sulfide Deposits, (ed..) H. Ohmoto and B.J. Skinner; Economic Geology, Monograph 5, p. 241–281.

Evans, D., and Kean, B., 2002. The Victoria Lake Supergroup, central Newfoundland – its definition, setting and volcanogenic massive sulphide mineralization; Newfoundland Department of Mines and Energy, Geological Survey, Open File NFLD/2790, 68 p.

Franklin, J., Gibson, H., Jonasson, I., and Galley, A., 2005. Volcanogenic massive sulphides, *In:* Economic Geology100th Anniversary Volume, (ed.) J.W. Hedenquist, J.F.H. Thompson, R.J. Goldfarb, and J.P. Richards; Society of Economic Geologists, Littleton, Colorado, p. 523–560.

Fraser, D., Giroux, G.H., Copeland, D.A., and Devine, C.A., 2012. Technical Report and Resource Minerals Estimate on the Lemarchant Deposit, South Tally Pond VMS Project, Central Newfoundland, Canada; NI 43-101 Technical Report prepared for Paragon Minerals Corporation, 132 p.

Gill, S.B., 2015. Mineralogy, Metal-Zoning, and Genesis of the Cambrian Zn-Pb-Cu-Ag-Au Lemarchant Volcanogenic Massive Sulfide (VMS) Deposit; M.Sc. thesis, Memorial University, St. John's, Newfoundland, 154 p.

Hackbarth, C.J. and Petersen, U., 1984. A fractional crystallization model for the deposition of argentian tetrahedrite; Economic Geology, v. 79, p. 448–460.

Hannington, M.D. and Scott, S.D., 1989. Sulfidation equilibria as guides to gold mineralization in volcanogenic massive sulfides: evidence from sulfide mineralogy and the composition of sphalerite; Economic Geology, v. 84, p. 1978–1995.

Hannington, M.D., Jonasson, I.R., Herzig, P.M., and Petersen, S., 1995. Physical and chemical processes of seafloor mineralization at mid-ocean ridges; *In:* Seafloor Hydrothermal Systems: Physical, Chemical, Biological, and Geological Interactions (ed.) S.E. Humphris, R.A. Zierenberg, L.S. Mullineaux, and R.E. Thomson; Geophysical Monograph, v. 91, p. 115–157.

Hannington, M.D., Poulsen, K.H., Thompson, J.F.H., and Sillitoe, R.H., 1999. Volcanogenic gold in the massive sulfide environment; Reviews in Economic Geology, v. 8, p. 325–356.

Hannington, M.D., de Ronde, C.D., and Petersen, S., 2005. Seafloor tectonics and submarine hydrothermal systems, *In:* Economic Geology 100th Anniversary Volume, (ed.) J.W. Hedenquist, J.F.H. Thompson, R.J. Goldfarb, and J.P. Richards; Society of Economic Geologists, Littleton, Colorado, p. 111–141.

Hannington, M.D., and Monecke, T., 2009. Modern submarine hydrothermal systems - A global perspective on distribution, size and tectonic settings, *In:* Submarine Volcanism and Mineralization: Modern through Ancient, (ed.) B. Cousens and S.J. Piercey; Geological Association of Canada, Mineral Deposits Division, Short Course Notes, v. 19, p. 91–146.

Hedenquist, J.W. and Lowenstern, J.B., 1994. The role of magmas in the formation of hydrothermal ore deposits; Nature, v. 370, p. 519–527.

Huston, D.L., 1999. Stable isotopes and their significance for understanding the genesis of volcanic-hosted massive sulphide deposits: a review; Reviews in Economic Geology, v. 8, p. 157–179.

Huston, D.L., 2000. Gold in volcanic-hosted massive sulphide deposits; distribution, genesis, and exploration; Reviews in Economic Geology, v. 13, p. 401–426.

Huston, D.L. and Large, R.R., 1989. A chemical model for the concentration of gold in volcanogenic massive sulphide deposits; Ore Geology Reviews, v. 4, p. 171–200.

Huston, D.L., Jablonski, W., and Sie, S., 1996. The distribution and mineral hosts of silver in eastern Australian volcanogenic massive sulphide deposits; The Canadian Mineralogist, v. 34, p. 529–546.

Kramers, J.D. and Tolstikhin, I.N., 1997. Two terrestrial lead isotope paradoxes, forward transport modeling, core formation and the history of the continental crust; Chemical Geology, v. 139, p. 75–110.

Large, R.R., 1977. Chemical evolution and zonation of massive sulphide deposits in volcanic terrains; Economic Geology, v. 72, p. 549-572.

Lode, S., Piercey, S. J., Devine, C. A., Layne, G. D., Piercey, G., and Hewa, L., 2014. Lithogeochemistry and sulphur isotopic composition of hydrothermal mudstones associated with the Lemarchant volcanogenic massive sulphide (VMS) deposit, Tally Pond Belt, Central Newfoundland, *In:* Abstracts; Geological Association of Canada, Newfoundland Spring Technical Meeting, v. 40, p. 20.

Longerich, H.P., Jackson, S.E., and Gunther, D., 1996. Inter-laboratory note: Laser ablation inductively coupled plasma mass spectrometric transient signal data acquisition and analyte concentration calculation; Journal of Analytical Atomic Spectrometry, v. 11, p. 899–904.

Lydon, J.W., 1996. Characteristics of volcanogenic massive sulphide deposits; interpretations in terms of hydrothermal convection systems and magmatic hydrothermal systems; Boletin Geologico y Minero, v. 107, p. 215–264.

Ohmoto, H. and Rye, R., 1979. Isotopes of sulphur and carbon, *In:* Geochemistry of Hydrothermal Ore Deposits, 2nd Edition, (ed.) H.L. Barnes; John Wiley & Sons, p. 509–567.

Ohmoto, H., Mizukami, M., Drummond, S., Eldridge, C., Pisutha-Arnond, V., and Lenagh, T., 1983. Chemical processes of Kuroko formation, *In:* The Kuroko and Related Volcanogenic Massive Sulfide Deposits, (ed.) H. Ohmoto and B.J. Skinner; Economic Geology, Monograph 5, p. 570–604.

Ohmoto, H., 1996. Formation of volcanogenic massive sulphide deposits; the Kuroko perspective; Ore Geology Reviews, v. 10, p. 135–177.

McNicoll, V., Squires, G., Kerr, A., and Moore, P., 2010. The Duck Pond and Boundary Cu-Zn deposits, Newfoundland; new insights into the ages of host rocks and the timing of VHMS mineralization; Canadian Journal of Earth Sciences, v. 47, p. 1481–1506.

Mercier-Langevin, P., Hannington, M., Dubé, B., and Bécu, V., 2011. The gold content of volcanogenic massive sulphide deposits; Mineralium Deposita, v. 46, p. 509–539.

Monecke, T., Petersen, S., and Hannington, M.D., 2014. Constraints on water depth of massive sulfide formation: evidence from modern seafloor hydrothermal systems in arc-related settings; Economic Geology, v. 109, p. 2079–2101.

Piercey, S.J. and Hinchey, J., 2012. Volcanogenic massive sulphide (VMS) deposits of the Central Mineral Belt, Newfoundland; Geological Association of Canada–Mineralogical Association of Canada Joint Annual Meeting, Field Trip Guidebook B, Newfoundland and Labrador Department of Natural Resources, Geological Survey, Open File NFLD/3173, 56 p.

Piercey, S.J., Squires, G.C., and Brace, T.D., 2014. Lithostratigraphic, hydrothermal, and tectonic setting of the Boundary volcanogenic massive sulphide deposit, Newfoundland Appalachians, Canada: Formation by subseafloor replacement in a Cambrian rifted arc; Economic Geology, v. 109, p. 661–687.

Pilote, J-L., Piercey, S.J., and Mercier-Langevin, P., 2014. Stratigraphy and hydrothermal alteration of the Ming Cu-Au volcanogenic massive-sulphide deposit, Baie Verte Peninsula, Newfoundland; Geological Survey of Canada, Current Research 2014-7, 18 p.

Pilote, J-L. and Piercey, S.J., 2013. Detailed volcano-stratigraphic relationships of the 1807 zone of the Cu-Au Ming volcanogenic massive sulphide (VMS) deposit, Baie Verte Peninsula, northern Newfoundland; Geological Survey of Canada, Current Research 2013-20, 17 p. doi: 10.4095/293128

Pisutha-Arnond, V. and Ohmoto, H., 1983. Thermal history, and chemical and isotopic compositions of the ore-forming fluids responsible for the Kuroko massive sulphide deposits in the Hokuroku District of Japan, *In:* The Kuroko and Related Volcanogenic Massive Sulfide Deposits, (ed.) H. Ohmoto and B.J. Skinner; Economic Geology, Monograph 5, p. 523–558.

Pollock, J., 2004. Geology and paleotectonic history of the Tally Pond Group, Dunnage zone, Newfoundland Appalachians: An integrated geochemical, geochronological, metallogenic and isotopic study of a Cambrian island arc along the Peri-Gondwanan margin of Iapetus; M.Sc. thesis, Memorial University, St. John's, Newfoundland, 420 p.

Poulsen, K.H. and Hannington, M.D., 1995. Volcanic-associated massive sulphide gold, *In:* Geology of Canada No. 8: Geology of Canadian Mineral Deposit Types, (ed.) O.R. Eckstrand, W.D. Sinclair, and R.I. Thorpe; Geological Society of America, Decade of North American Geology (DNAG), Part 1, p. 183–196.

Rogers, N., van Staal, C.R., McNicoll, V., Pollock, J., Zagorevski, A., and Whalen, J., 2006. Neoproterozoic and Cambrian arc magmatism along the eastern margin of the Victoria Lake Supergroup: A remnant of Ganderian basement in central Newfoundland?; Precambrian Research, v. 147, p. 320–341.

Sakai, H. and Dickson, F., 1978. Experimental determination of the rate and equilibrium fractionation factors of sulphur isotope exchange between sulphate and sulphide in slightly acid solutions at 300ºC and 1000 bars; Earth and Planetary Science Letters, v. 39, p. 151–161.

Sakai, H., Des Marais, D., Ueda, A., and Moore, J., 1984. Concentrations and isotope ratios of carbon, nitrogen and sulphur in ocean-floor basalts; Geochimica et Cosmochimica Acta, v. 48, p. 2433–2441.

Santaguida, F. and Hannington, M., 1993. Preliminary results on gold mineralization in volcanogenic massive sulphide deposits, central Newfoundland, *In:* Current Research, (ed..) C.P.G. Pereira, D.G. Walsh, and R.F. Blackwood; Government of Newfoundland and Labrador, Department of Mines and Energy, Geological Survey Branch, Report 93-01, p. 373–381.

Santaguida, F. and Hannington, M., 1996. Characteristics of gold mineralization in volcanogenic massive sulphide deposits of the Notre Dame Bay area, central Newfoundland; Canadian Journal of Earth Sciences, v. 33, p. 316–334.

Scott, S. and Barnes, H., 1971. Sphalerite geothermometry and geobarometry; Economic Geology, v. 66, p. 653–669.

Seal, R.R., 2006. Sulphur isotope geochemistry of sulphide minerals; Reviews in Mineralogy and Geochemistry, v. 61, p. 633–677.

Shanks, W., 2001. Stable isotopes in seafloor hydrothermal systems: vent fluids, hydrothermal deposits, hydrothermal alteration, and microbial processes; Reviews in Mineralogy and Geochemistry, v. 43, p. 469–525.

Sillitoe, R.H., Hannington, M.D., and Thompson, J.F.H., 1996. High sulfidation deposits in the volcanogenic massive sulfide environment; Economic Geology, v. 91, p. 204–212.

Squires, G. and Moore, P., 2004. Volcanogenic massive sulphide environments of the Tally Pond Volcanics and adjacent area: Geological, lithogeochemical and geochronological results, *In:* Current Research; Newfoundland and Labrador Department of Natural Resources, Geological Survey, Report 04-1, p. 63–91.

Stacey, J.S. and Kramers, J., 1975. Approximation of terrestrial lead isotope evolution by a two-stage model; Earth and Planetary Science Letters, v. 26, p. 207–221.

Swinden, H. and Kean, B., 1988. The volcanogenic sulphide districts of central Newfoundland: A guidebook and reference manual for volcanogenic sulphide deposits in the Early Paleozoic oceanic volcanic terranes of central Newfoundland; Geological Association of Canada, Mineral Deposits Division, p. 2–27.

Ueda, A. and Sakai, H., 1984. Sulphur isotope study of Quaternary volcanic rocks from the Japanese Islands Arc; Geochimica et Cosmochimica Acta, v. 48, p. 1837–1848.

van Staal, C.R., Dewey, J.F., Niocaill, C.M., and McKerrow, W.S., 1998. The Cambrian-Silurian tectonic evolution of the northern Appalachians and British Caledonides: History of a complex, west and southwest Pacific-type segment of Iapetus; Geological Society, London, Special Publications, v. 143, p. 197–242. doi:10.1144/GSL.SP.1998.143.01.17

van Staal, C. and Barr, S., 2012. Lithospheric architecture and tectonic evolution of the Canadian Appalachians and associated Atlantic margin, Chapter 2 *In:* Tectonic Styles in Canada Revisited: the LITHOPROBE perspective, (ed.) J.A. Percival, F.A. Cook, and R.M. Clowes; Geological Association of Canada, Special Paper 49, p. 41–95.

White, N.C. and Hedenquist, J.W., 1995. Epithermal gold deposits: styles, characteristics and exploration; Society of Economic Geologists newsletter, v. 23, p. 9–13.

Williams, H., 1979. Appalachian orogen in Canada; Canadian Journal of Earth Sciences, v. 16, p. 792–807.

Zagorevski, A., Van Staal, C.R., McNicoll, V., and Rogers, N., 2007. Upper Cambrian to upper Ordovician peri-Gondwanan island arc activity in the Victoria Lake Supergroup, Central Newfoundland: tectonic development of the northern Ganderian margin; American Journal of Science, v. 307, p. 339–370.